Time dependent magnetization and stiffness measurements in thin superconducting rings

Bornovski Matan

Technion

December 7, 2025

Outline

Motivation

- Iron-based superconductors, in particular $FeSe_{0.5}Te_{0.5}$, show:
  - Strong correlations.
  - Complex multiband electronic structure.
  - Nontrivial topology and unconventional pairing.
- Peri et al. (2023)
  - Bulk single crystal.
  - Stiffness (ρ_s) vs. T showed a **knee**.
  - M vs H did **not** show the same knee.
  - Disagreement with H_{c1} measurements.

Peri et al. (2023) "knee" effect

Proposed explanations:

1. Electronic nematic phase transition.
2. Surface superconductivity (different T_c for bulk vs surface).
3. Multiple Fermi surfaces (multigap superconductivity).
4. Sample geometry.

Leading questions

- Is the knee feature:
  - intrinsic to $FeSe_{0.5}Te_{0.5}$?
  - related to Ring geometry?
  - related to Stoichiometric inhomogeneity?
  - related to Experimental limitations?
- Strategy:
  - Use thin film $FeSe_{0.5}Te_{0.5}$ grown by PLD.
  - Measure both M vs. H and using Stiffnessometer.
  - Control: different material with similar geometry.

Superconductivity basics

- Superconducting phase:
  - Meissner effect (expulsion of magnetic field).
  - Zero resistance.
- Two main theories:
  - BCS (microscopic).
  - Ginzburg–Landau (phenomenological).
- Type I vs Type II:
  - Type I: single critical field H_c.
  - Type II: mixed state between H_{c1} and H_{c2} with vortices.

Superconducting length scales and GL relations

- **London penetration depth** λ_L:
  - Characteristic decay length of magnetic field inside a superconductor.
- **Coherence length** ξ:
  - Scale over which the order parameter varies significantly.

$$\mu_0 H_{c1} \approx \frac{\Phi_0}{4\pi\lambda^2} \ln\left(\frac{\lambda}{\xi}\right)$$

Order parameter and stiffness

- GL order parameter:

$$\Psi(\vec{r}) = |\Psi(\vec{r})| e^{i\phi(\vec{r})}$$

- London equation:

$$\vec{J}_s = -\rho_s \left(\vec{A}_{\text{tot}} - \frac{\Phi_0}{2\pi} \nabla\phi \right)$$

- Measuring $\rho_s(T)$ gives direct access to the superfluid density:

$$\rho_s = \frac{|\Psi|^2 e^{*2}}{m^*} = \frac{1}{\mu_0 \lambda_L^2}$$

BCS gap and two-gap model

- Below T_c an energy gap $\Delta(T)$ opens at the Fermi surface.
- For s-wave:

$$\frac{\lambda^{-2}(T)}{\lambda^{-2}(0)} = 1 + 2\int_{\Delta(T)}^{\infty} \partial_E f \, \frac{E\,dE}{\sqrt{E^2 - \Delta^2(T)}}$$

  along with a closed approximate form.
- Two-gap s-wave model:

$$\rho_T(T) = w\,\rho_{\Delta_1}(T) + (1-w)\,\rho_{\Delta_2}(T)$$

- A knee in stiffness can naturally arise from multigap behavior.

Thin films and Pearl length

- For thin films with $d \ll \lambda_L$:

$$\Lambda = \frac{2\lambda_L^2}{d}$$

  known as the Pearl length.
- Field screening is not longer exponential - vortices may have long range correlations.
- Stiffnessometer directly probes the 2D stiffness through Λ.

$FeSe_{0.5}Te_{0.5}$: structure

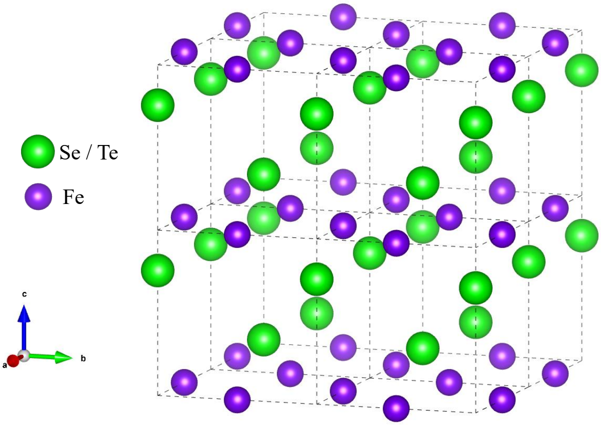

Figure 1: Crystal structure of $FeSe_{0.5}Te_{0.5}$.

$FeSe_{0.5}Te_{0.5}$: topology & pairing

- DFT: multiple electron and hole pockets, band inversion.
- ARPES: confirms band inversion and surface states.
- Experiments (STM, μSR, Andreev spectroscopy) indicate:
  - Two superconducting gaps.
  - Possible unconventional pairing (e.g. $s + id$).
  - Candidate for topological superconductivity and Majorana modes.

Stiffnessometer concept

- Superconducting annulus threaded by a long excitation coil.
- DC current in the coil:

$$\vec{A} = \frac{\mu_0 n I}{r}\hat{\varphi}$$

  while H is confined inside the solenoid.
- The annulus sees a pure vector potential $\vec{A}$:
  - Induces supercurrents (Meissner effect).
  - Generates a magnetic moment measured by SQUID.
- From $m(I)$ we extract the stiffness and ξ.

Measurement protocols: ZGFC

Zero-Gauge-Field Cooling (ZGFC):

Step	Action
1	Reach desired base temperature.
2	Drive desired current in excitation coil.
3	Measure magnetic moment.

- Sets $\nabla\phi = 0$ in London equation (fixed gauge).
- Probes response to pure vector potential at fixed T.

System setup: MPMS3 Stiffnessometer configuration

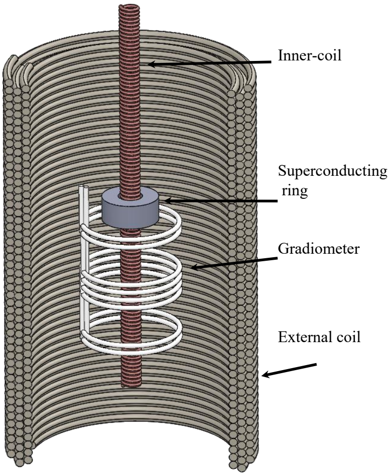

Figure 2: MPMS3 in Stiffnessometer configuration.

Sample holder: Stiffnessometer

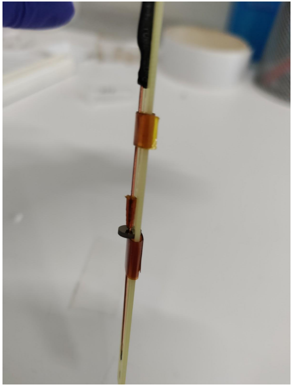

Figure 3: Stiffnessometer sample holder: excitation coil + LAO ring with film.

- Copper excitation coil threading the superconducting ring.
- $LaAlO_3$ substrate with $Fe_ySe_xTe_{1-x}$ film patterned as a ring.

Sample holder: DC-field measurements

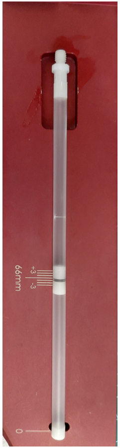

Figure 4: Sample holder for external field measurements.

- Straw-bead assembly holding the ring.
- Bare LAO substrate background measured and subtracted.

SQUID magnetometer and modes

Measurement modes:

- DC mode: scan sample along z, fit dipole profile $\Rightarrow m$.
- VSM mode: oscillate sample, measure oscillating signal $\Rightarrow m$.

Both modes give consistent magnetization measurements.

ZFC and FC DC-field protocols

Zero-Field Cool (ZFC):

- Heat to $15\,\mathrm{K}$, null field.
- Cool to base T.
- Apply field, then measure $m(t)$.

Field Cool (FC):

- Heat to $15\,\mathrm{K}$.
- Apply field, cool to base T.
- Measure $m(t)$.

- ZFC: minimizes trapped flux and history effects.
- FC: retains flux history, sensitive to pinning and trapping.

Measurement protocols: GFC

Gauge-Field Cooling (GFC):

Step	Action
1	Drive desired current in excitation coil.
2	Cool to base temperature.
3	Set excitation-coil current to zero.
4	Measure magnetic moment.

- Enforces gauge-invariant combination:

$$\vec{A}_{tot} - \frac{\Phi_0}{2\pi}\nabla\phi = 0$$

- Probes trapped phase winding and persistent currents.

Extracting ξ from critical flux

- Start from GL free energy in thin-ring approximation.
- Assume separable order parameter $\Psi = \psi(r)\Theta(\theta)$.
- Minimize free energy $\Rightarrow$ critical flux condition:

$$\frac{\Phi_c}{\Phi_0} \approx \frac{r_{\text{out}}}{\xi}$$

- Break in the linear $m(I)$ response gives Φ_c and thus $\xi(T)$.

Extracting λ and stiffness

- Use London equation in 2D:

$$\nabla^2 \vec{A}_{SC} = \mu_0 \rho_s (\vec{A}_{SC} + \vec{A}_{EC})$$

- Solve PDE for an annulus using FreeFEM++ with cylindrical symmetry.
- At pickup loop radius R_{pl}:

$$A(R_{pl}) = C \frac{m}{I}$$

- From $\frac{m}{I}$ and geometry:
  - Extract $A(R_{pl})$.
  - Obtain Λ and then λ_L via $\Lambda = 2\lambda_L^2/d$.
  - Get $\rho_s(T) \propto \lambda^{-2}(T)$.

Magnetic response vs temperature

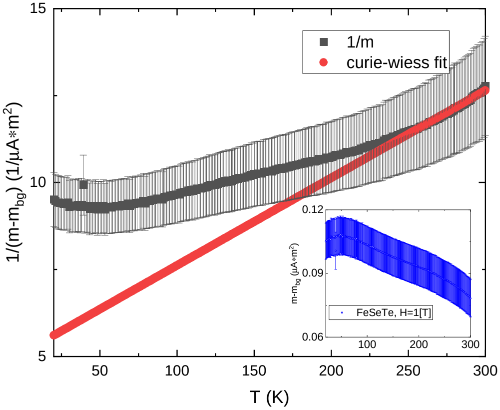

Figure 5: Inset M vs T $H = 1(\mathrm{T})$, background-subtracted.

Magnetic response vs temperature: key points

- Measure film + LAO at $H = 1\,\text{T}$; subtract LAO.
- Maximum signal $\sim 0.1\,\mu\text{A}\cdot\text{m}^2$.
- Inverse magnetization vs T:
  - Deviates strongly from Curie–Weiss behavior.
  - Fit to high-T region gives effective $T_c < 0$ (antiferromagnetic-like), but global behavior not Curie–Weiss.
- Conclusion: dominant response cannot be ascribed simply to excess Fe; this contribution is neglected in further analysis.

Stiffnessometer $m(I)$

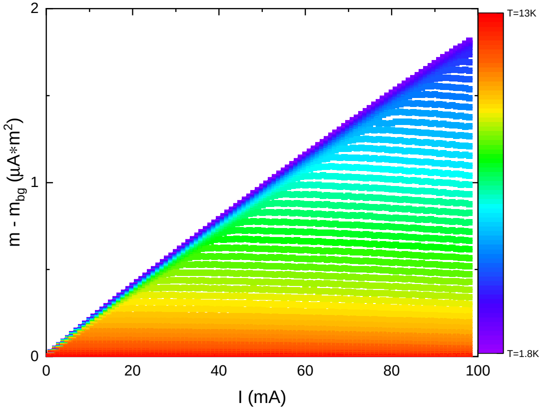

Figure 6: Excitation-coil current dependence of m for different T.

Critical current and low excitation current slope vs. T

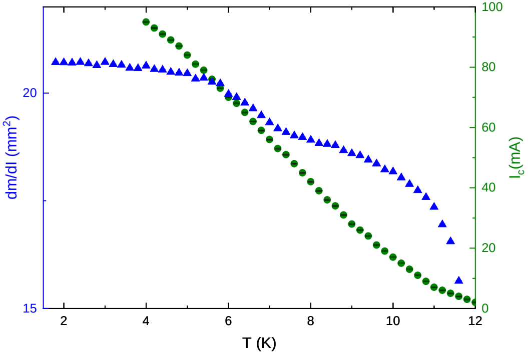

Figure 7: $\frac{dm}{dI}$ and I_c vs. T.

- $\frac{dm}{dI}$:
  - Monotonically decreases with T.
  - Exhibits a knee near $\sim 7\,$K.
  - Drops sharply near T_c.
- $I_c(T)$:
  - Smoothly decreases as $T \to T_c$.

Inverse Pearl length and inverse coherence length

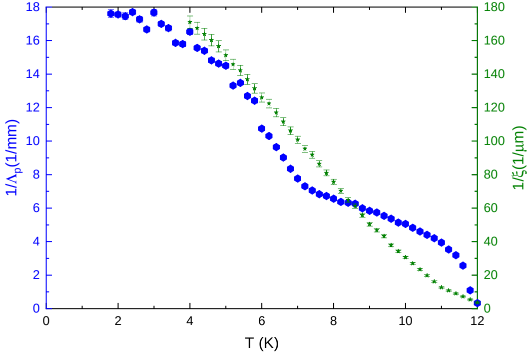

Figure 8: $\Lambda_p^{-1}(T)$, $\xi^{-1}(T)$.

- $\Lambda_p^{-1}(T)$:
  - Monotonic with T.
  - Pronounced knee around $7\,\mathrm{K}$.
- $\xi^{-1}(T)$:
  - Smooth evolution without a clear knee.

Normalized stiffness vs two-gap model

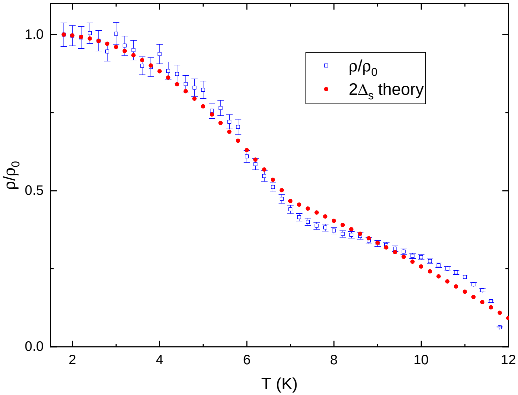

Figure 9: Normalized stiffness vs two-gap model.

Normalized stiffness fits well to two-gap s-wave model:

- Two gaps with $T_{c,1} = 7(\mathrm{K})$, $T_{c,2} = 13.4(\mathrm{K})$.
- Supports multiband origin of the knee.
- fails to capture behavior close to T_c

Gap values vs literature

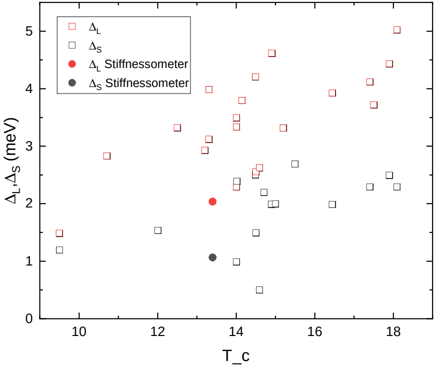

Figure 10: Gap magnitudes vs T_c with present data overlaid on XXX.

- Our extracted gaps roughly follow literature trends for Δ_L and Δ_S, but with deviations.
- Possible reasons:
  - Thin film vs bulk crystals.
  - Degraded or different T_c.
  - Simplifying assumption of negligible interband coupling in model.

$H_{c1}(T)$ from $\lambda(T)$ and $\xi(T)$

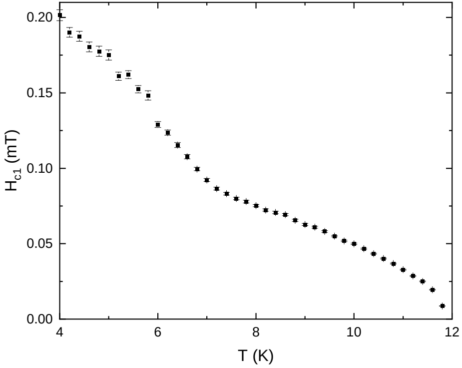

Figure 11: $H_{c1}(T)$ obtained from $\lambda(T)$ and $\xi(T)$.

- H_{c1} decreases monotonically with T, as expected with observed "knee".
- H_{c1} values in the mT range.

Time dependence: ZFC vs FC vs GFC

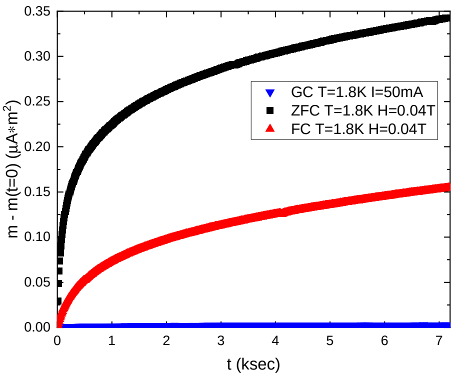

Figure 12: Relative magnetization vs time for ZFC, FC, and GC protocols.

Unexpected time dependence

- ZFC and FC:
  - Clear positive, nonlinear change in magnetization over time.
  - Strongly non-linear in $\ln t$.
  - Sometimes exhibit sign changes in the moment.
- GC:
  - Only a small positive change.
- This type of time-dependent behavior was not reported previously for $Fe_ySe_xTe_{1-x}$.

ZFC protocol: short-time behavior

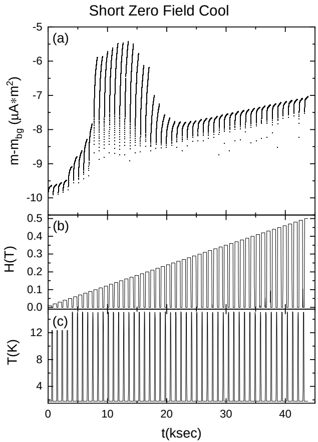

Figure 13: ZFC: $m(t)$, $H(t)$ and $T(t)$ at $T = 1.8$ K.

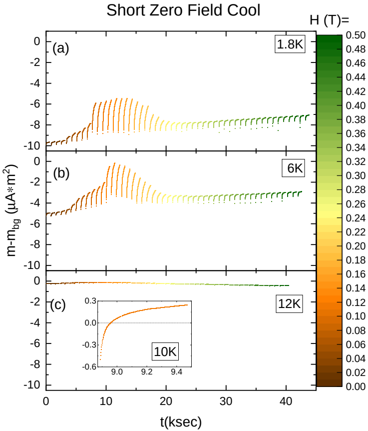

Figure 14: ZFC: $m(t)$ at $T = 1.8, 6, 12$ K for various fields.

ZFC: time dependence summary

- For all T and H:
  - Nonlinear evolution of $m(t)$.
  - Recurring pattern of short and long saturation times vs H.
- Increasing T:
  - Initial moment moves toward zero.
  - Saturation time becomes shorter.
- In some cases (specific T and H):
  - $m(t)$ switches sign.

ZFC: long-time behavior

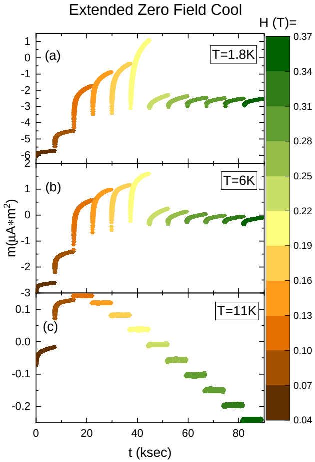

Figure 15: ZFC: extended $m(t)$ over $\Delta t = 7.2$ ksec.

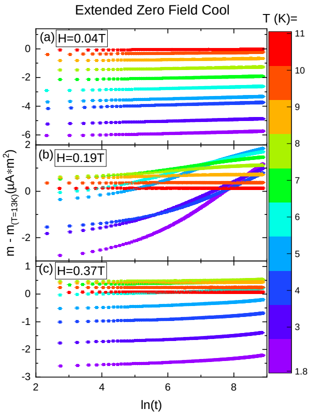

Figure 16: ZFC: superconducting moment vs $\ln t$ for three fields.

FC protocol: short-time behavior

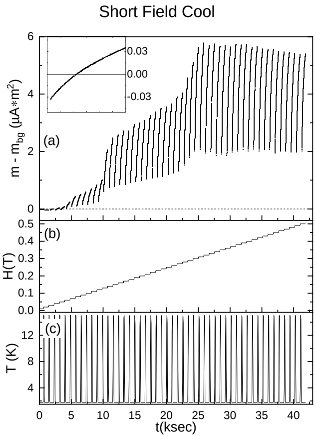

Figure 17: FC: $m(t)$, $H(t)$ and $T(t)$ at $T = 1.8$ K.

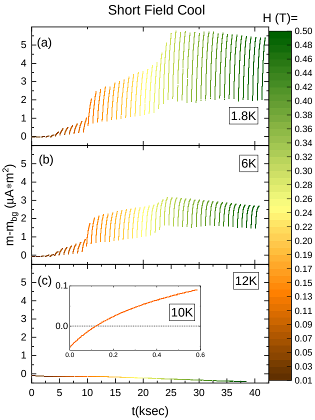

Figure 18: FC: $m(t)$ at $T = 1.8, 6, 12$ K, various fields.

FC: long-time behavior

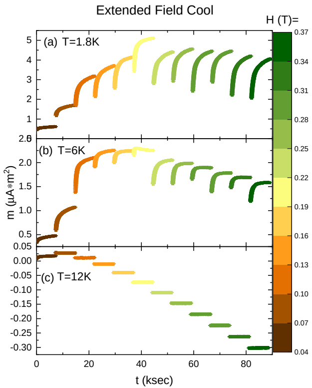

Figure 19: FC: extended $m(t)$ over $\Delta t = 7.2$ ksec.

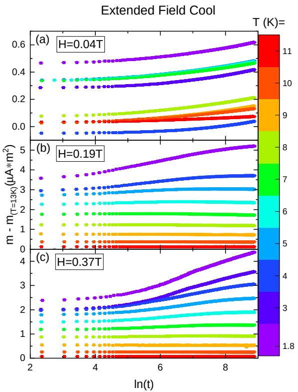

Figure 20: FC: superconducting moment vs $\ln t$ for three fields.

Vector potential modulation

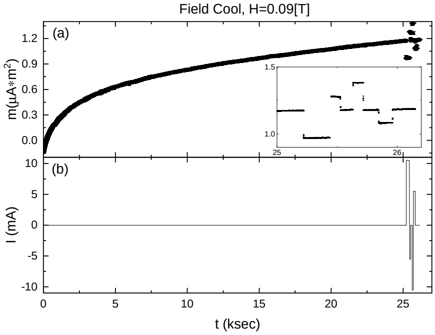

Figure 21: FC: response to modulated excitation coil current at $T = 1.8$ K, $H = 0.09$ T.

- Magnetic moment changes sign over long times.
- When vector potential is modulated:
  - Response is persistent.
  - Proportional to applied vector potential.
- Confirms superconducting origin of the observed signal.

Comparison sample: NbTiN ring

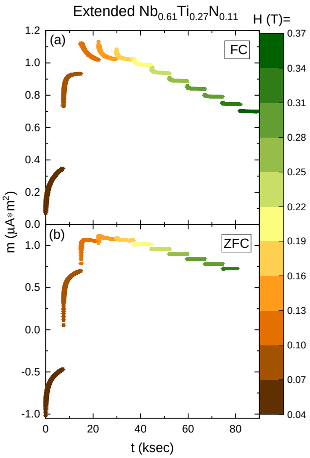

NbTiN ring with similar geometry shows:

- Clear time-dependent magnetization in both FC and ZFC.
- Different detailed behavior from FeSeTe, but with:
  - Positive responses tending toward saturation.
  - Sign changes and non-linear $m(\ln t)$.

Figure 22: $Nb_{0.61}Ti_{0.27}N_{0.11}$ ring: FC and ZFC

Conclusions: stiffness and "knee"

- Stiffnessometer on thin $FeSe_{0.5}Te_{0.5}$ rings:
  - Reproduces the **knee** in stiffness vs T, around $\sim 7\,$K.
  - $\xi^{-1}(T)$ evolves smoothly without a pronounced "knee".
- Two-gap s-wave BCS model:
  - Captures main features of normalized stiffness.
  - Suggests multiband origin of the knee.

Conclusions: Geometric origin of time dependence

- NbTiN ring with similar geometry shows:
  - Clear time-dependent magnetization in both FC and ZFC.
  - Different detailed behavior from FeSeTe, but with:
    - Positive responses tending toward saturation.
    - Sign changes and non-linear $m(\ln t)$.
- Indicates that:
  - Time-dependence is not unique to FeSeTe.
  - Likely has a strong **geometric** component.

Conclusions: time-dependent magnetization

- Both ZFC and FC protocols show:
  - Strong, non-linear $m(\ln t)$ behavior.
  - Positive time evolution, sometimes including sign changes.
- GC protocol shows only small changes.
- Vector-potential modulation confirms superconducting origin of the signal.
- Comparison with NbTiN ring:
  - Time-dependence is seen in a different superconductor with similar geometry.
  - Points to a **geometric** effect of the annular ring on flux dynamics.

Outlook

- Improve modeling:
  - Include interband coupling and realistic band structure.
  - Quantitative modeling of vortex dynamics in annular geometry and edge effects.
- Experimental directions:
  - Systematic geometry variations (width, thickness, inner radius).
  - Compare different materials (s-wave, d-wave, topological).
  - perform scanning/MFM measurements along edges and in radial direction to determine the role of vortex dynamics in the time dependence.

Thank you!

Questions?